ELSEVIER

Catalysis Today 23 (1995) 365–370

CATALYSIS TODAY

Quantum chemical approach to the interpretation of the STM tunneling mechanism: semiempirical calculations on the electronic structures of silica/silicon clusters

Masaharu Komiyama *, Yasumi Iwashita

Department of Chemistry, Yamanashi University, Takeda, Kofu 400, Japan

Abstract

The mechanism of scanning tunneling microscopy (STM) observations of a surface of a silicon oxide (silica) thin film grown on crystalline silicon and its silica/silicon interface were investigated by means of semiempirical quantum chemical calculations. Cluster models representing the silica/silicon system were constructed, and their electronic structures were calculated. A previously postulated STM observation mechanism was examined in terms of the calculated energy levels of the clusters and the spatial distributions of their electron orbitals.

1. Introduction

Scanning tunneling microscopy (STM) is an attractive tool for the study of heterogeneous solid catalyst surfaces. High spatial resolution, high environmental freedom and the spectroscopic capabilities inherent to it are all desirable characteristics in a catalyst characterization technique. Its application in the field of catalysis, however, has been largely limited to electroconductive materials, due to its operating principles which require a tunneling current to flow between the probe tip and the sample surface. Widely used catalysts, however, often contain nonconductive materials such as silica or alumina, and for the study of such nonconductive material surfaces, atomic force microscopy (AFM) is often employed. AFM relies on the atomic forces exerted between the atoms on the probe tip and those on the sample surface and thus does not require electrical conductivity on the sample. Due to this working principle, however, AFM provides only topographic images of sample surfaces and no spectroscopic information.

In this context, it is of practical interest to establish a procedure which enables the STM study of nonconductive material surfaces. For silica, which is one of the commonly used catalyst support materials, we have shown that it is possible to perform STM on a thin (ca. 0.6 nm thick) silica film grown on a crystalline silicon surface [1]. We were also able to obtain STM images of platinum ultrafine particles deposited on this thin silica film surface [2,3]. STM images on alumina and Pt/alumina have also been obtained [3,4].

The STM observations of the above silica/silicon system were found to be critically dependent on the tunneling conditions, particularly on the tunneling voltage V_t. Depending on the value of V_t employed, STM/STS images attributable to the

* Corresponding author.

SSDI 0920-5861(94)00150-2

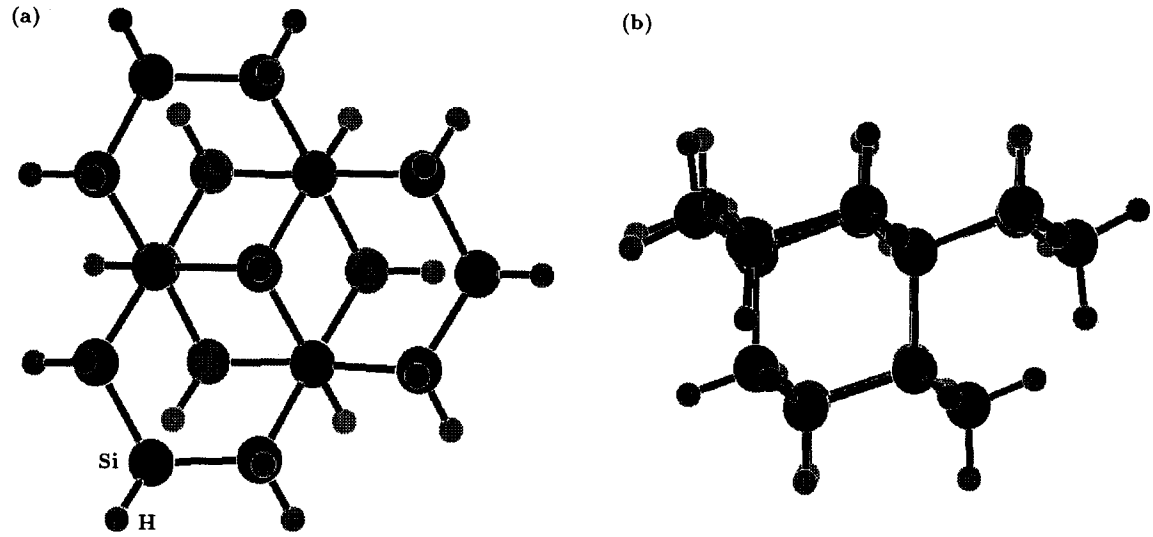

Fig. 1. Hydrogen-terminated silicon cluster made of 19 Si atoms. (a) Top view and (b) side view.

silica surface or the silica/silicon interface were obtained [1]. The present paper aims at interpreting and explaining the STM observation mechanism of this silica/silicon surface and the interface by means of semiempirical quantum chemical calculations on model silica/silicon clusters.

2. Methods

Semiempirical quantum chemical calculations on model thin-film silica/silicon systems were performed using the MOPAC program (version 6) installed on a SUN SPARKstation IPX. Firstly a hydrogen-terminated single crystal silicon surface was modelled by hydrogen-terminated silicon clusters made of 19 silicon atoms. The cluster geometry was optimized using PM3 Hamiltonian. Thin silica film grown on a silicon surface was modelled by substituting hydrogens on one face of the above cluster with hydroxyl, siloxy or silicate groups. Here the geometry of silicon substrate was fixed to that of the above optimized hydrogen-terminated silicon cluster, and only the geometries of the newly added groups were optimized. The cluster electronic structures and the orbital distributions were calculated along with infrared spectra and other pertinent properties.

Table 1
Si–Si distances for the optimized hydrogen-terminated silicon cluster (Fig. 1) and the Si bulk [5]

	Si–Si distance (nm)
Calculated	0.235–0.238
Crystallographic	0.235

3. Results and discussion

3.1. Hydrogen-terminated silicon surface

Firstly a silicon cluster with its surface dangling bonds terminated with hydrogen was constructed as a model of a hydrogen-terminated silicon surface. Fig. 1 shows the constructed and fully optimized cluster that contain 19 Si atoms. The adequacy of this cluster as a model for the actual system was examined by comparing three calculated quantities, the geometry of the silicon substrate, its infrared (IR) spectrum and its energy band gap, with their respective experimental values available.

Table 1 compares the PM3-optimized Si–Si distances in the cluster with crystallographically determined distances in the silicon bulk [5]. While the cluster Si–Si distance showed a tendency to relax at the cluster periphery, it was found

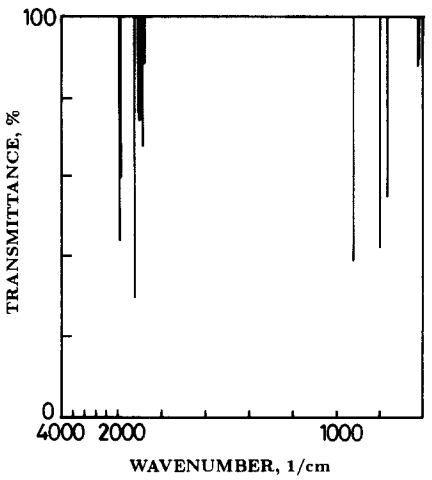

Fig. 2. Infrared spectrum calculated for the hydrogen-terminated silicon cluster shown in Fig. 1.

that the calculated Si–Si distance was very close to that of bulk Si crystal. Together with the fact that the optimized cluster shows almost perfect silicon crystallographic structure (Fig. 1), it may be considered that the present cluster is a good model of a hydrogen-terminated silicon surface.

The calculated IR spectrum of the above cluster, shown in Fig. 2, indicates that the Si–H stretching vibrations appear between 1900 and 2000 cm^{-1}. The published experimental spectrum [6] obtained from a hydrogen-terminated single crystal silicon surface shows the vibrations between 2050 and 2150 cm^{-1}. The correspondence between the two appears to be satisfactory, again indicating that the present model is a reasonable approximation to the actual system. It should be noted, however, that IR mode frequencies are more sensitive to the local environment than to the long-range structure, and thus good correspondence is generally expected between the model cluster calculation and that actually measured.

Table 2 lists the calculated molecular orbital energy levels of the cluster shown in Fig. 1. It shows that the highest occupied molecular orbital (HOMO) of this cluster is placed at −8.4 eV and its lowest unoccupied MO (LUMO) at −2.6 eV. The difference between these two levels may be considered as the energy gap for the hydrogen-terminated silicon surface it represents, and it amounts to 5.8 eV. While an experimental band-gap value for the hydrogen-terminated silicon surface is not available, the experimental value for the silicon bulk band gap is ca. 1.1 eV [7]. Although an exact comparison between these two values may not be appropriate, it is obvious that the cluster calculation shows a much wider 'band gap' than its bulk counterpart, and this is attributed to the size effect on the electronic structure. In general, the band gap is known to increase with decreasing cluster size, and thus the use of cluster models in lieu of a true bulk treatment will always overestimate the band-gap value.

With the calculated energy levels listed in Table 2, one may explain the mechanism of the STM observation as follows: in STM if one applies a bias voltage between the sample and the tip, the applied bias effectively produces a difference in Fermi energy between the sample and the tip of that amount, which otherwise is at the same level. Thus if a negative bias voltage is applied to the tip, electrons tunnel from the valence band of the tip into the unoccupied states in the sample located

Table 2
Calculated molecular orbital energy levels for the hydrogen-terminated silicon cluster shown in Fig. 1

No.	Eigenvalues (eV)
⋮	
50	−8.893
51	−8.442
52	−8.406 HOMO
53	−2.597 LUMO
54	−2.553
55	−2.548
56	−2.327
57	−2.146
58	−2.142
59	−2.126
60	−2.037
61	−2.030
62	−1.927
63	−1.919
64	−1.677
65	−1.613
66	−1.478
67	−1.468
68	−1.166
⋮	

at the same energy levels. With the present cluster, a 4 V negative bias voltage, for example, could induce tunnelling of electrons from the tip into the cluster MOs number 53 through 65, assuming its Fermi level was at the center of the HOMO and LUMO. What would then be imaged by the STM at this bias voltage would be the superposition of the spatial distribution of these 13 molecular orbitals.

3.2. *Thin silica film on a silicon surface*

One face of the above hydrogen-terminated silicon cluster was 'oxidized' by substituting the hydrogen atoms on the face with hydroxyl, siloxy or silicate groups, as shown in Fig. 3, in order to simulate the thin-film silica grown on a silicon substrate surface. Their calculated energy band gaps are listed in Table 3.

It is found in Table 3 that the band-gap values, or the differences between the HOMOs and LUMOs, decrease when the hydrogen-terminated surface is oxidized. This apparently contradicts the common expectation that the oxide has a wider band gap compared to its unoxidized semiconductor precursor. This contradiction may be accounted for by the following two factors. Firstly, this may partly be a reflection of the cluster size effect on its electronic structure. Our 'oxidation' progressively increases the total number of atoms involved in each cluster as found in Table 3. As discussed earlier, increasing the size of the model cluster tends to bring the overestimated band-gap value closer to its bulk value.

Table 3
Band-gap values of the silica/silicon clusters

	Band gap (eV)	No. of atoms in the cluster
Hydrogen-terminated	5.8	47
Hydroxy-terminated	5.3	54
Siloxy terminated	4.9	57
Silicate-terminated	5.0	69

A second factor for the apparent band-gap decrease may lie in the fact that the present clusters in effect consist of two phases, viz., part oxidized and part unoxidized, and not all the calculated levels belong to the oxidized phase. Close examination of the spatial distribution of each MO in each cluster indicates that this separation becomes apparent in the silicate-terminated cluster. Fig. 4 exemplifies the spatial distribution of a few of its MOs. The silicate-terminated cluster MOs above LUMO (at -1.9 eV) up to -0.6 eV are mostly localized around substrate Si atoms, and only after energy levels of -0.6 eV do MOs start to have a significant contribution from oxidized layers. For reasons which are not known, this separation does not appear in the filled states, as may be found in Fig. 4, and all the levels below HOMO have more or less equal contributions from both the oxidized and unoxidized cluster atoms.

Thus for the silicate-terminated cluster we have essentially two LUMOs, one for the unoxidized

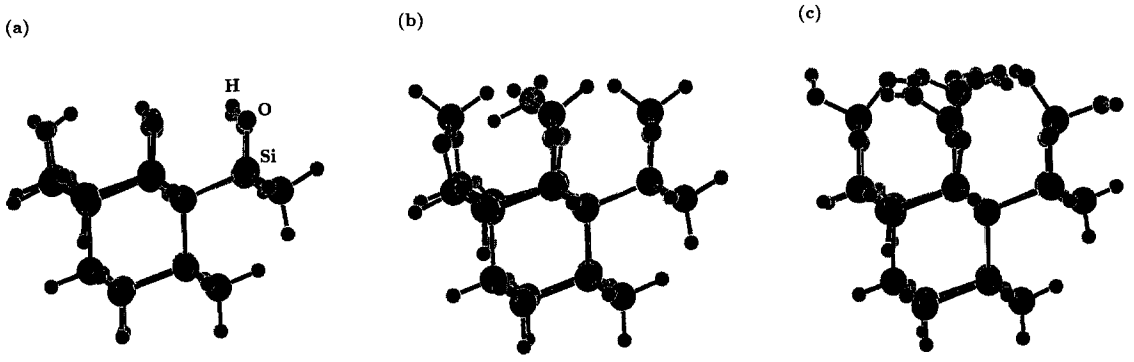

Fig. 3. Hydrogen-terminated silicon cluster made of 19 Si atoms, with one face being terminated by hydroxyl (a), siloxy (b) and silicate groups (c).

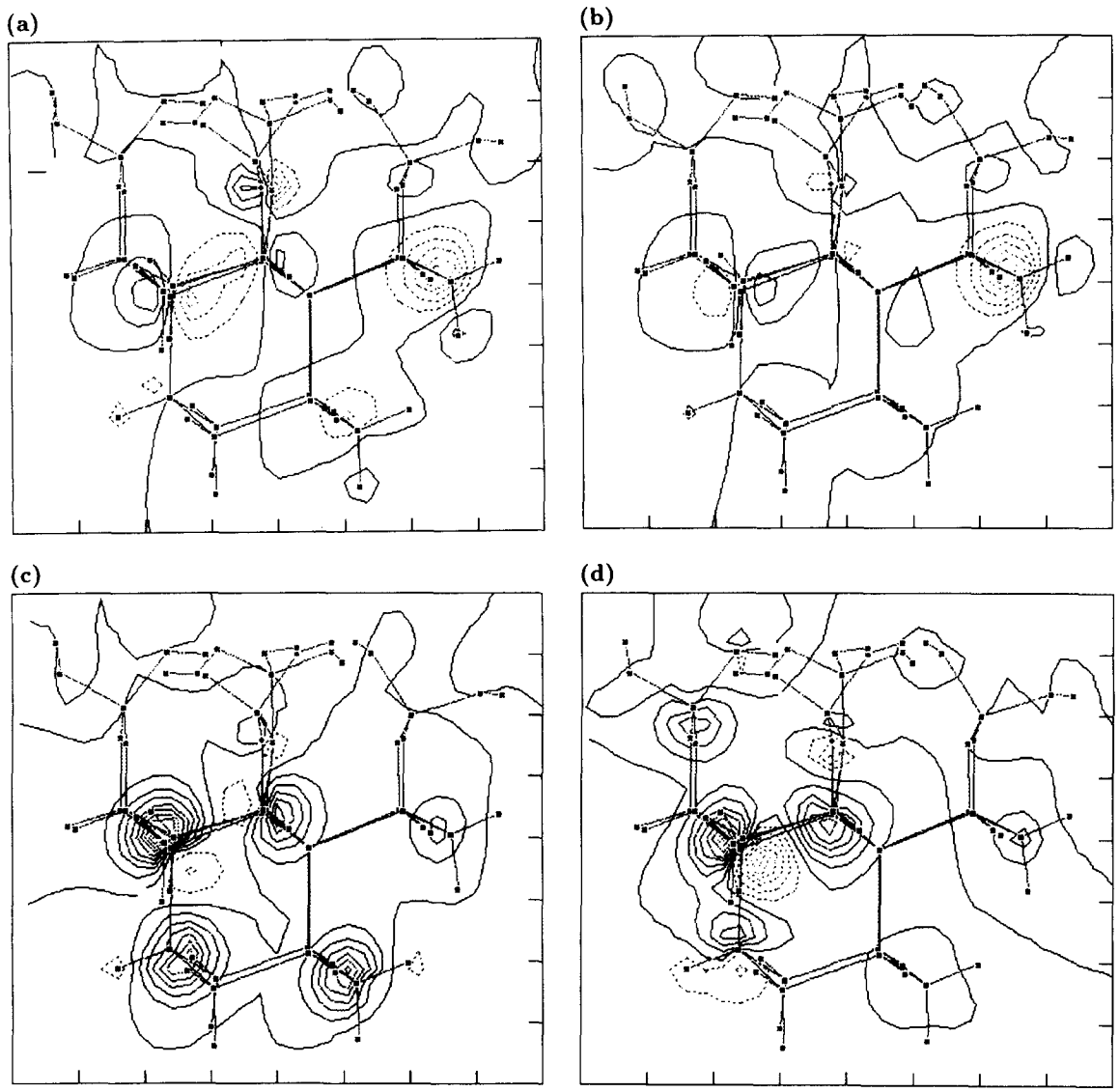

Fig. 4. Spatial distributions of several molecular orbitals around the Fermi edge of the siliate-terminated silicon cluster. (a) At −7.8 eV, (b) −7.0 eV (HOMO), (c) −1.5 eV and (d) −0.5 eV.

and the other for the oxidized phase. Apparently the high-energy LUMO is the one to be compared with bulk oxides, and this places the calculated energy band gap for the oxide layer at 6.4 eV, closer to the experimental bulk oxide value of 8.5 eV.

From the above discussion it is clear that the electron tunneling mechanism for those samples whose surfaces are oxidized should be considered in two phases: one for the oxide phase and the other for the unoxidized phase. Thus if one applies bias voltages high enough to include the oxidized LUMO level, the electrons can tunnel into those oxide phase levels, and the STM images obtained will be those of the oxidized surface. Electrons may also tunnel into unoxidized phase levels at such biases, but since these levels are spatially located further into the surface than those of the oxidized phase levels, their contributions to the STM image will be minimal.

The lowest-lying unoccupied oxidized levels for the silicate-terminated cluster are found at

−0.6 eV. Taking the Fermi level at the middle of each band gap, this would require a V_t of ca. 3.3 eV for the STM observation of the oxide surface. These values are still lower than the actual bias voltage of 4 V employed in the previously reported STM measurements of the thin silica surface [1], thus justifying the interpretation of these STM images reported earlier. It should be noted that the present model is very close to the actual system in terms of oxide thickness, for the actual system has only 0.6 nm thick oxide [1], which translates into only two layers of silicate.

What happens if one employs V_t below the lowest-lying oxidized levels? Here the electrons tunnel into unoxidized Si states rather than the oxidized states, and since they are located below the oxidized layer, this results in the observation of the silica/silicon interface rather than the silica surface, the silica layer being transparent to the tunneling electrons. In this case the oxide layer has to be very thin, otherwise the tip will be driven into the oxide surface and will become sufficiently close for electrons to tunnel into the interface.

4. Conclusions

Semiempirical calculations were performed on clusters that model the hydrogen-terminated silicon surface and the silica thin film grown on a crystalline silicon substrate. The electronic structure calculations showed that the silica/silicon system could be considered to comprise of two phases, the oxide and its substrate. From the calculated energy levels, the conditions appropriate for STM imaging of the oxide surface and the silica/silicon interface were identified. The present calculation justifies the previously published mechanism and the interpretation of STM/STS imaging of the thin-film silica/silicon system.

Acknowledgements

The assistance of Ms. I. Okuda in operating EWSs and the MOPAC software is acknowledged.

References

[1] M. Komiyama, M. Kirino and H. Kurokawa, Jpn. J. Appl. Phys., 32 (1993) 2934.
[2] M. Komiyama and M. Kirino, Chem. Lett., (1992) 2301.
[3] M. Komiyama, M. Kirino and H. Kurokawa, J. Vacuum Sci. Technol. B, 12 (1994) 1869.
[4] M. Komiyama and H. Kurokawa, Chem. Lett., (1994) 1421.
[5] R.W.G. Wyckoff, Crystal Structure, Interscience, New York, 1963.
[6] S. Watanabe, M. Shigeno, N. Nakayama and T. Ito, Jpn. J. Appl. Phys., 30 (1991) 3575.
[7] D.A. Baglee, in N.G. Einspruch (Editor), VLSI Handbook, Academic Press, New York, 1985, p. 385.